

Estimation of the direct radiative forcing due to sulfate and soot aerosols

By GUNNAR MYHRE*, FRODE STORDAL¹, KNUT RESTAD and IVAR S. A. ISAKSEN,
Department of Geophysics, University of Oslo, Norway; ¹Also at Norwegian Institute for Air Research (NILU), Norway

(Manuscript received 13 November 1997; in final form 17 June 1998)

ABSTRACT

The direct radiative forcings due to tropospheric sulfate and fossil fuel soot aerosols are calculated. The change in the atmospheric sulfate since preindustrial time is taken from a recent three-dimensional chemistry transport model calculation. A multistream radiative transfer code and observed atmospheric input data is used. The direct radiative forcing due to sulfate is calculated to -0.32 W/m^2 . Our results for global and annual mean radiative forcing have been compared with results from other model studies. We have assumed a linear relationship between the concentration of fossil fuel soot and sulfate aerosols. The resulting radiative forcing due to soot particles is 0.16 W/m^2 . Two types of mixtures of sulfate and soot are further assumed. The calculated single scattering albedo is compared to observations.

1. Introduction

Climatic effects of aerosols have been subject of much research over the last few years, and several global estimates of the direct radiative effects due to aerosols have been made (Charlson et al., 1991; Kiehl and Briegleb, 1993; Taylor and Penner, 1994; Boucher and Anderson, 1995; Haywood and Shine, 1995; Haywood et al., 1997a; Chuang et al., 1997; Feichter et al., 1997). The magnitude of the indirect aerosol effect is very uncertain (IPCC, 1995), but not discussed further in this study.

In the context of climate research most attention has been paid to sulfate aerosols among the tropospheric aerosols. Most of the recent estimates yield a cooling below 0.5 W/m^2 from the sulfate aerosols of a global scale (Haywood et al., 1997a; Chuang et al., 1997; Feichter et al., 1997) due to scattering of solar radiation. Fossil fuel soot in contrast to the sulfate aerosols, also absorb solar radiation at all wavelengths. Haywood et al. (1997a) show that

when clouds are taken into account the importance of soot increases. They estimate a warming of about 0.2 W/m^2 . Haywood et al. (1997a) and Hansen et al. (1997) show that a mixture of soot and sulfate aerosols may further increase the importance of the absorption by soot aerosols.

The concept radiative forcing is introduced as a simple tool to compare different radiatively active components that influence the radiative balance. It is used e.g., in the IPCC assessments (IPCC, 1995; IPCC, 1990). The radiative forcing is usually calculated at the tropopause level after allowing the stratosphere to adjust to radiative equilibrium. Ramaswamy and Chen (1997) and Hansen et al., (1997) show that the radiative forcing at the tropopause is a relatively good measure of the change in the surface temperature for different radiatively active components, however Hansen et al., (1997) show that the climate response depends also on spatial effects related to each individual radiatively active component.

In this work we present new estimates of the radiative forcing due to sulfate aerosols and soot

* Corresponding author.

aerosols. We use a new sulfate distribution calculated with a 3-dimensional (3D) chemistry-transport-model (CTM) (Restad et al., 1998) for sulfate. The sulfate distribution is also used to establish a fossil fuel soot distribution. Unlike most other studies of the radiative forcing due to aerosols, we use a multistream radiative transfer code. Geographical variation of the aerosol forcing is investigated, and calculations are performed to identify the regions in which the radiative forcing is most sensitive to changes in sulfate and soot concentration. Radiative transfer calculations of mixtures of sulfate and soot are also performed, and single scattering albedo from the mixtures are compared to observations. We also include a comparison with earlier model calculations of the radiative forcing due to aerosols.

2. Models and methods

2.1. Sulfate data

The sulfate distribution we have used in this work is from Restad et al. (1998). A 3D CTM (Berntsen and Isaksen, 1997) with a horizontal resolution of 10° in longitude and 8° in latitude and a vertical resolution of 9 layers was used to calculate this distribution. The adopted SO_2 emissions were based on the Geia data base (Benkovitz, 1996). In addition volcanic emissions as given by Stoiber (1987) were included, with a source of 8.7 TgS/yr which was found to affect the upper tropospheric sulfate levels. The emission of DMS was taken from Bates et al. (1992), which is the same as the emissions used in the studies by Langner and Rodhe (1991) and Feichter et al. (1996).

The CTM calculations were performed with a sulfur chemistry scheme including a simplified parameterization of heterogeneous oxidation and oxidation of SO_2 in gas phase by OH. The parameterization of the sulfate formation in the liquid phase, the wet and liquid phase removal was calculated in a way similar to Rodhe and Isaksen (1980). It was assumed that the process is irreversible and that it occurs in connection with cloud formation. The data for removal were scaled to the optical thickness data from a general circulation model to give longitudinal and temporal distribution (Berntsen and Isaksen, 1997; Restad et al., 1998). The OH distribution was taken from

a version of the 3D model including ozone chemistry (Berntsen and Isaksen, 1997). Two calculations were performed, one including only natural emissions of sulphur dioxide and one including both natural and anthropogenic emissions. The anthropogenic emission data for sulphur dioxide represented 1985 conditions.

The modelled sulfate is in reasonable good agreement with surface observations. It reproduces for instance the observed long range transport of sulfate from polluted regions to the Arctic during the winter season rather well (Restad et al., 1998). This model feature is in better agreement with observations than what was obtained in Langner and Rodhe (1991) and in Feichter et al. (1996). Although the annual agreement with surface observations is reasonably good in marine background atmosphere in the calculations by Restad et al. (1998), sulfate levels seem to be somewhat underestimated in the tropics and at higher latitudes during summer, up to 50%. Possible explanations are underestimated aqueous phase transfer of SO_2 in the boundary layer (SO_2 levels were somewhat high), or underestimated sulfate formation from DMS.

2.2. Radiative properties of aerosols

The radiative properties of the aerosols are in this work estimated taking into account three factors; the specific extinction coefficient, the asymmetry factor, and the single scattering albedo. Calculations using Mie theory are performed to calculate the radiative properties. Several parameters are necessary in the Mie calculations, as e.g., the refractive indexes and size distribution (Kiehl and Briegleb, (1993)) in order to describe the three factors above. The dry sulfate is described only as ammonium sulfate, as several studies have shown that the direct sulfate aerosol forcing is relatively insensitive to whether the aerosols consist of $(\text{NH}_4)_2\text{SO}_4$, NH_4HSO_4 , or H_2SO_4 (Nemesure et al., 1995; Pilinis et al., 1995; Kiehl and Briegleb, 1993; Haywood et al. 1997a). In the calculations of the radiative properties of ammonium sulfate and soot aerosols we follow to a large degree the procedure in Haywood et al. (1997a) and Haywood and Shine (1997). Refractive indexes are taken from Toon et al. (1976) and WCP (1986) for ammonium sulfate and soot respectively. The size distributions are

assumed to be lognormal, with geometric mean radii of $0.05\ \mu\text{m}$ for dry ammonium sulfate and $0.0118\ \mu\text{m}$ for soot aerosols. Both aerosols species have a geometric standard deviation of 2.0 (Kiehl and Briegleb, 1993).

Ammonium sulfate aerosols are hygroscopic, and the parametrization in Fitzgerald (1975) is used for relative humidities above 81% to describe the growth of the aerosols. Large areas at high latitudes (above 60° in the southern hemisphere and 70° in the northern hemisphere) near the surface have relative humidities above 81%, and the maximum relative humidity is above 95%. The ammonium sulfate aerosols are assumed to be dry at relative humidities below 30%. Between relative humidities of 30% and 81%, a linear growth factor for the particle radius is assumed. Volume weighting of the ammonium sulfate and

water refractive indexes are performed. For each 0.5% relative humidity Mie calculations are performed using hydrated geometric mean radii from Fitzgerald (1975) in the lognormal size distribution (Haywood et al., 1997a). Fig.1 shows the results of the Mie calculations for ammonium sulfate particles for several relative humidities. For high relative humidities the specific extinction coefficient decreases at short wavelength and increases with increasing wavelength compared to the dry ammonium sulfate aerosol. The specific extinction coefficient is highest for particles for a radius close to the wavelength of the solar radiation. At wavelengths below about $1\ \mu\text{m}$ the increased radius for high relative humidity reduces specific extinction coefficient, and vice versa at wavelengths above about $1\ \mu\text{m}$. The results shown in Fig. 1 are for the specific extinction coefficient,

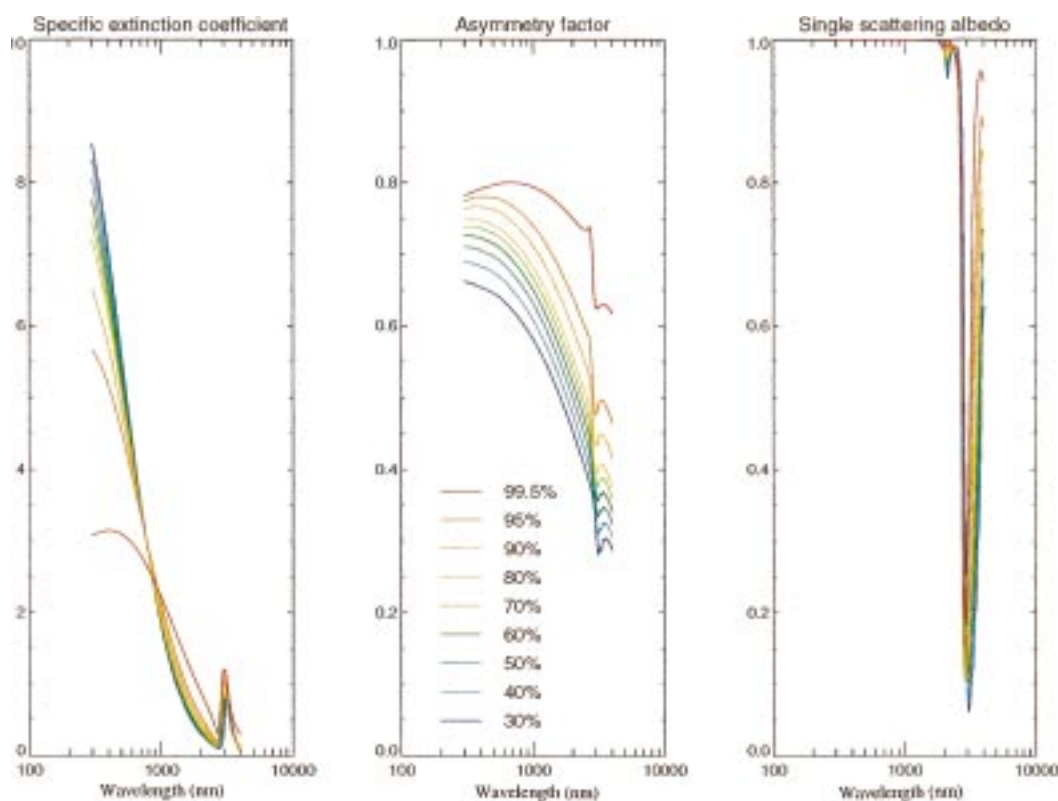


Fig. 1. Specific extinction coefficient, asymmetry factor, and single scattering albedo for ammonium sulfate for several relative humidities. The colour code is the same in all panels. Notice that our results for the specific extinction coefficient are given relative to the total mass of the particle (sulfate + water), whereas previous results have most frequently been given relative to the mass of sulfate only.

and are given per unit mass. The mass of the aerosols increases substantially with increasing relative humidity, e.g., for relative humidity of 99.5% the mass of the wet ammonium sulfate aerosols is a factor 30–40 higher than that of a dry aerosol. Correspondingly, the optical depth increases by more than a factor 10. Therefore the increase in relative humidity influences the optical depth in two different ways: (i) through increase in the size of the particles which reduce the specific extinction coefficient, and (ii) through increase in the mass of water, which dominates over (i).

The asymmetry factor increases with increasing relative humidity. This means that the larger particles will scatter more radiation into the forward direction and reduce the effect of larger aerosol particles somewhat. The single scattering albedo increases somewhat at long wavelengths in the solar spectrum but this is of minor importance for the radiative effects of the ammonium sulfate aerosols, as there is a low specific extinction coefficient and also low incoming solar energy at these wavelengths.

We assume that the fossil fuel soot aerosols are hydrophobic, therefore no growth with increasing relative humidity is taken into account. In lack of emission data for soot and a model describing the transformation, transport, and deposition of soot, we use a linear relationship between concentrations of soot and ammonium sulfate. The mass ratio between fossil fuel soot and ammonium sulfate is chosen to be 0.075. This assumption is based on limited information and uncertainties therein are discussed in Haywood et al. (1997a). We have adopted the procedure for calculation of radiative properties of soot from Haywood and Shine (1997). Our results are very similar to their results and therefore not shown here.

2.3. Radiation scheme and atmospheric input data

A model using the discrete ordinate method (Stamnes et al., 1988) is used in the radiative transfer calculations. The calculations are performed with 8 streams. The scattering from aerosols and clouds are therefore calculated in a more accurate way than the usual 2-stream approximation. We have performed test experiments with our model in a 2-stream mode, finding that differences between the 8-stream and 2-stream approaches could lead to differences up to 20%.

The model includes absorption by H_2O , CO_2 , O_2 , and O_3 , Rayleigh scattering, and absorption and scattering by clouds and aerosols. Absorption data for H_2O , CO_2 , O_2 , and O_3 in the infrared region are taken from the HITRAN-92 database (Rothman et al., 1992), where temperature dependence is included for H_2O and CO_2 . Cross sections for O_2 and O_3 in the ultraviolet and visible region and Rayleigh scattering are from WMO (1985). The extra terrestrial solar spectrum is taken from Frohlich and London (1986). Three cloud layers are assumed in the calculations, where no overlap between the cloud layers are taken into account. We follow the approach of Lacis and Mishchenko (1995) in the calculations of the specific extinction coefficient, the asymmetry parameter, and the single scattering albedo in the presence of several scattering media (e.g., for clouds and aerosols). The spectral resolution varies over the solar spectrum, with a relatively high resolution below $2\ \mu\text{m}$ and a lower spectral resolution above $2\ \mu\text{m}$, altogether dividing the solar spectrum into about 70 intervals. Calculations using this spectral resolution are in good agreement with control calculations which we have performed using a spectral resolution of 1 nm, with a deviation less than 1–2%. Thermal infrared calculations of the aerosols have not been performed as the infrared contribution was shown in Haywood et al. (1997a) to be less than 3% of the total ammonium sulfate aerosol forcing.

Relative humidities, temperatures, albedo, and cloud distributions are monthly averaged. Relative humidities and temperatures are taken from ECMWF (European Centre for Medium-Range Weather Forecasts). The atmospheric distribution of ozone is based on satellite and sonde observations (Liang and Wang, 1991). Surface albedo and cloud data are taken from ISCCP (International Satellite Cloud Climatology Project) (Rossow and Schiffer, 1991). Haywood and Shine (1997) show that the radiative forcing due to the aerosols is highly dependent upon zenith angle, therefore we have performed radiative transfer calculations every third hour in order to obtain diurnal averages representing the conditions of each of the four months January, April, July, and October. For short-wave forcing due to change in tropospheric ozone the selection of these 4 months has been shown to represent within 1% accuracy the 12 months of the year (Berntsen et al., 1997).

3. Results of the radiative transfer calculations

3.1. Ammonium sulfate

The global and annual mean radiative forcing at the tropopause level is -0.32 W/m^2 , see Table 1. The instantaneous radiative forcing at the tropopause level is only 1% stronger than the adjusted forcing. The calculations of the adjusted forcing are performed with a thermal infrared broad band model (Myhre and Stordal, 1997). Previous studies have used the instantaneous radiative forcing at the top of the atmosphere (TOA), which in our work is 2–3% weaker than the adjusted forcing at the tropopause. The weaker forcing at the TOA is due to absorption of scattered radiation in the stratosphere. This absorbed radiation increases the temperature in the stratosphere. Thereby the thermal infrared emission from the stratosphere down to the troposphere/surface system increases. The difference between the adjusted radiative forcing at the tropopause and the instantaneous

forcing at the TOA is small compared to the deviations between previous aerosol radiative forcing estimates based on different models.

Plate 1 shows the annual mean global distribution of the radiative forcing due to ammonium sulfate. As found also in the previous studies, the forcing is mostly localized in eastern part of north America, Europe (particularly southern part), and east Asia. In the southern hemisphere local maxima over south America and south Africa around 30° are calculated. The maximum forcing is over southern Europe, and is about -2.5 W/m^2 annually, and close to -5 W/m^2 in July.

As described in Haywood and Shine (1997) there is no simple relationship between the radiative forcing in cloudy regions and the total forcing, the clear sky forcing, and the cloud amount. Using the procedure from Haywood et al. (1997a), where the total forcing was subtracted from the forcing from the cloud free regions, we find that the forcing from cloudy regions is -0.087 W/m^2 or about 27% of the total sulfate forcing. This contribution from the cloudy regions are substantially higher than in Haywood et al. (1997a), but probably closer to Boucher and Anderson (1995) and Coakley et al. (1983).

To study the effect of the growth of the aerosols in humid regions we have performed a calculation for dry ammonium sulfate. The results show that the growth factor increases the forcing with only a factor of 1.2, which is much lower than in the calculations of Haywood et al. (1997a) and

Table 1. *Aerosol radiative forcing*

Aerosol type	Global (W/m^2)	NH (W/m^2)	SH (W/m^2)
ammonium sulfate	-0.32	-0.55	-0.08
soot	0.16	0.28	0.03
external mixture	-0.16	-0.26	-0.05
internal mixture	0.10	0.19	0.01

NH: northern hemisphere; SH southern hemisphere.

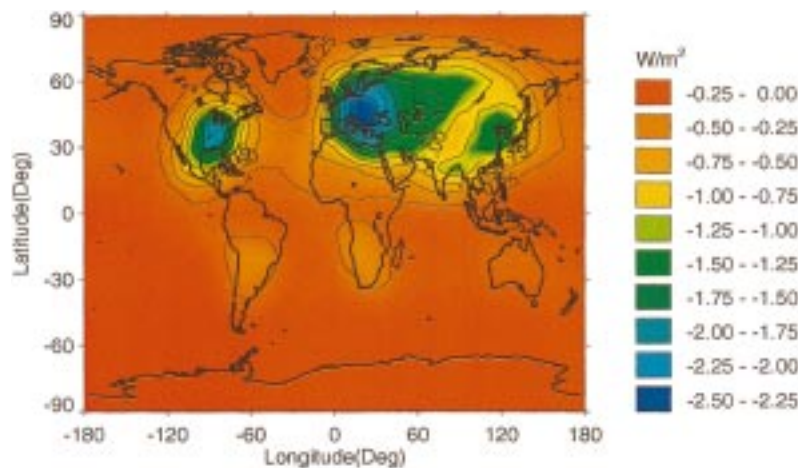


Plate 1. Yearly average radiative forcing due to sulfate aerosols.

Boucher and Anderson (1995). Haywood et al. (1997b) showed that due to a large nonlinear effect in the growth of particles with relative humidity, subgrid scale variation can be important for the sulfate forcing. Monthly mean relative humidities are used in our calculations, and variation of relative humidity during the month would probably increase the sulfate forcing. The effect of averaging of relative humidity on the radiative forcing due to aerosols both in spatial and temporal resolution is subject of a present study.

The seasonal variation in radiative forcing is rather large with almost a factor 2 stronger forcing in July compared to January, with values of -0.46 and -0.24 W/m^2 , respectively. The seasonal variation is in good agreement with what is found in Chuang et al. (1997).

3.2. Soot

Global annual mean radiative forcing due to soot has been calculated to 0.16 W/m^2 as shown in Table 1. Like sulfate, the difference between the radiative forcing due to soot at the tropopause and at the TOA is small. Likewise, the effect of stratospheric temperature adjustment is negligible.

The annual mean radiative forcing due to soot aerosols is shown in Plate 2. The soot aerosols give a positive radiative forcing as the absorption effect dominates the scattering effect. The maximum forcing is displaced somewhat eastward compared to the maximum sulfate forcing, with

high forcing over the whole Eurasia continent. Local maxima are also found similar to for sulfate over eastern part of North America and south east Asia. Maximum radiative forcing is about 1 W/m^2 for the annual mean and more than 2 W/m^2 in July. At high latitudes the radiative forcing for soot are relatively stronger than for sulfate. The seasonal variation is large with 0.10 W/m^2 in January and 0.25 W/m^2 in July.

The clouds increase the soot forcing substantially. Using the procedure described above for sulfate, we obtain a forcing which is 0.05 W/m^2 without clouds compared to 0.16 W/m^2 when clouds are included. Low clouds contribute with about half of the forcing in cloudy regions. Absorbing particles are very efficient over high albedo areas, as clouds, making the low clouds most important for soot aerosols. The clear sky forcing due to soot is 0.12 W/m^2 .

3.3. Geographical variations of the radiative forcing

From the geographical distributions of the radiative forcing due to sulfate and soot it was found large regional gradients. The regions that were found to be most affected by radiative perturbations differ in the two cases. To investigate the role of variability in atmospheric parameters as humidity, clouds and solar zenith angle on the forcing we have performed global experiments using constant vertical distribution of aerosols for

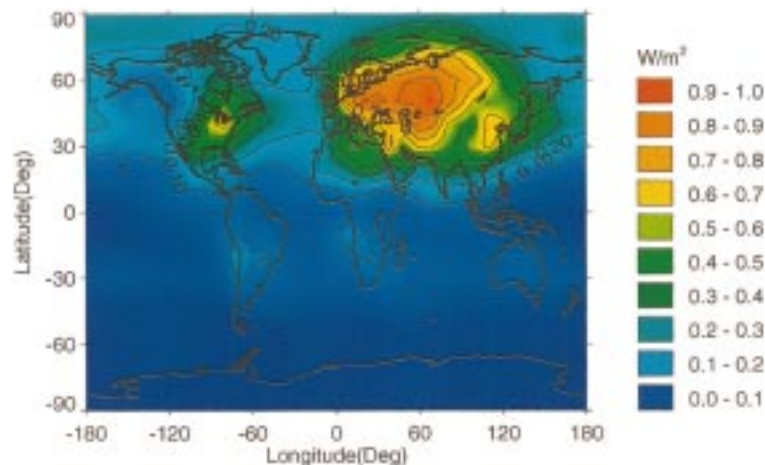


Plate 2. Yearly average radiative forcing due to soot aerosols.

the entire globe. Two profiles were used; one which describes global averages in the case of natural emissions only and one in which also anthropogenic emissions are included, as shown in Fig. 2. We have compared the distribution of sulfate used in this work to the results of Langer and Rodhe (1991), as shown by Haywood et al. (1997a). We found that globally and annually averaged concentrations used in this work were higher than those of Langer and Rodhe (1991), by up to 35% in the lower troposphere and up to 20% between 600 and 200 hPa. However, in the 800–600 hPa region, the sulfate concentrations used in this work is 15% lower than in Langer and Rodhe (1991).

Plate 3 shows the radiative forcing due to

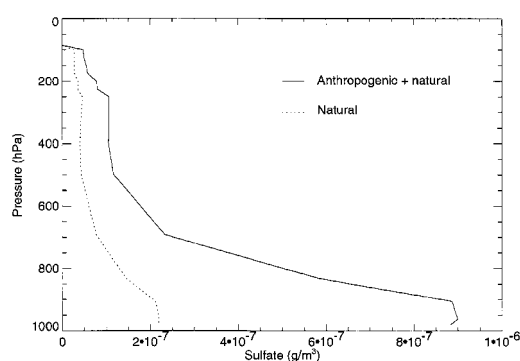


Fig. 2. Global mean vertical distribution of natural and anthropogenic ammonium-sulfate.

anthropogenic sulfate aerosols using the constant global mean sulfate amount. Haywood and Shine (1997) found that sulfate aerosol forcing is weak over regions with high albedo and that the soot forcing is strong over regions with high albedo. This is also found in our results. The sulfate forcing is weak over regions with deserts or large cloud amounts. Strong forcing is found over regions with small cloud amounts and low surface albedo, as over oceans, especially eastern Pacific ocean 0–30°S, eastern coasts of south and central America, south Africa and south east Asia, and partly the Mediterranean ocean. The maximum forcing due to sulfate over the south of Europe using the 3D CTM calculated distribution is a combination of high mass of sulfate and favourable conditions for high forcing.

The radiative forcing due to soot assuming constant soot amount over the globe is shown in Plate 4. Generally, the soot forcing is strong when the sulfate forcing is weak and vice versa, with very high values over the Arctic and especially Antarctica. In the regions with strong soot forcing over land the surface albedo is relatively high. Clouds increase the soot forcing in general, but over high surface albedo areas as in the Arctic, clouds reduce the soot radiative forcing. The variation of the forcing over oceans is mostly due to clouds. The west coasts of south and central America, south Africa, and Australia all have large

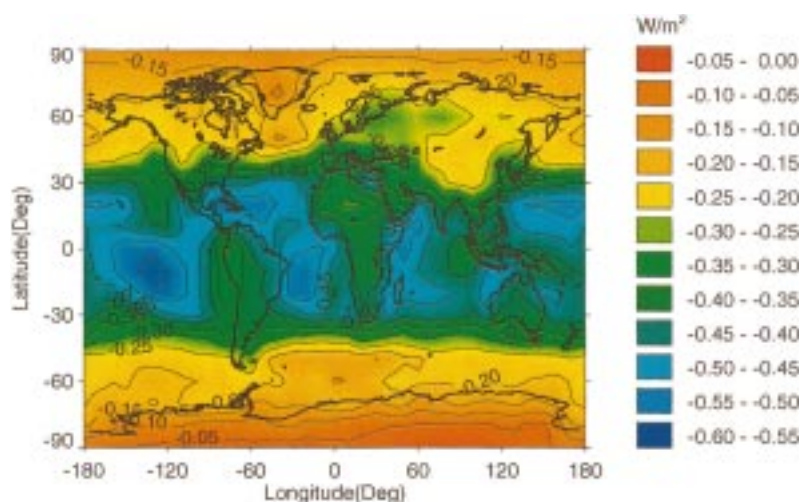


Plate 3. Yearly average radiative forcing due to sulfate aerosols using a constant global mean sulfate concentration.

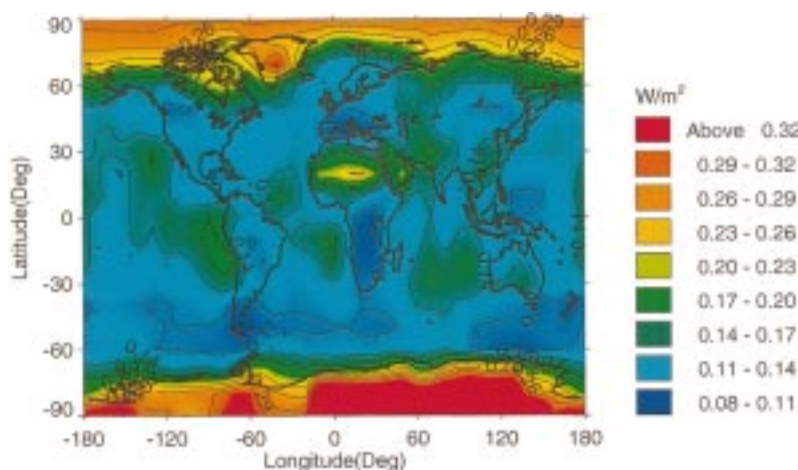


Plate 4. Yearly average radiative forcing due to soot aerosols using a constant global mean soot concentration.

forcing. In these regions there are also high amounts of low clouds and small amounts of middle and high clouds. At 60°S the cloud amount is very high, but a large fraction of these clouds are middle and high clouds. Therefore, the clouds are above most of the soot, giving a smaller forcing. The maximum soot forcing shown in Plate 2 coincides with one of the regions with most favourable conditions for high soot forcing.

The global seasonal variation in the radiative forcing of soot and sulfate aerosols using the global average vertical profile is small. However, there is a strong seasonal variation in the forcing in each of the two hemispheres, with about 50% higher forcing in summer than in winter. Therefore, the calculated seasonal variation in the radiative forcing using the sulfate distribution from the CTM is a combination of more solar radiation in July than in January in the northern hemisphere and larger sulfate burden in July than in January.

3.4. External mixture of ammonium sulfate and soot

An external mixture of sulfate and soot is assumed to consist of sulfate and soot aerosols as separate particles. Calculations of external mixture of sulfate and soot as one calculation differ by less than 3% from separate calculation of sulfate and soot. The global radiative forcing is -0.16 W/m^2 as shown in Table 1.

Plate 5 shows the annual mean spatial distribution of the radiative forcing for the external mixing. Two distinct maxima (negative forcing) areas in southern Europe and east northern America are very pronounced, whereas the maximum over south east Asia resulting from the sulfate particles is not so pronounced. The western part of Asia has weak forcing which coincides with the high soot forcing in this area. At high latitudes the external mixing radiative forcing is positive. The seasonal cycle shows large variation with -0.09 W/m^2 in April and -0.20 W/m^2 in July.

3.5. Internal mixture of ammonium sulfate and soot

In an internal mixture of sulfate and soot they are assumed to constitute one particle. Radiative properties of the particle are different from those of an external mixture and new Mie calculations are necessary. An internal mixture is shown to give lower single scattering albedo than an external mixture (Ackerman and Toon, 1981; Haywood et al., 1997a).

New Mie calculations are performed where refractive indexes from sulfate and soot are volume weighted. When the relative humidity is above 30% water is also taken into account, again using volume weighting of the refractive indexes. We have adopted a procedure for an internal mixture particle of sulfate and soot similar to what is used in Haywood et al. (1997a). This follows up the procedures that we have used for wet sulfate

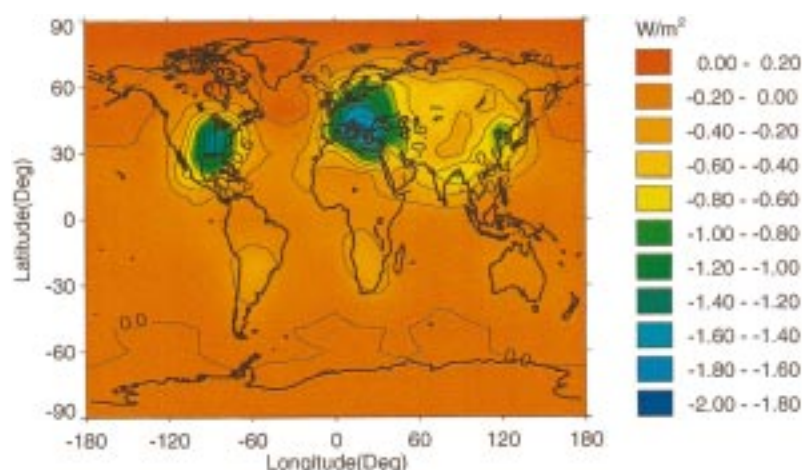


Plate 5. Yearly average radiative forcing due to an external mixture of sulfate and soot aerosols.

particles. The results of the Mie calculation of the internal mixing for several relative humidities are shown in Fig.3. For the specific extinction coefficient and the asymmetry factor there are only small changes from the sulfate calculations. The specific extinction for a dry internal mixing aerosol is only slightly higher than the specific extinction for a dry sulfate aerosol. The asymmetry factor is somewhat higher in the dry internal mixture than for the dry sulfate for short wavelengths. For high relative humidities the differences are very small. However for the single scattering albedo the differences between the internal mixture and the sulfate is relatively large, especially for the dry aerosols. For high relative humidity the radiative properties are more similar to the radiative properties of water which has single scattering albedo of 1 below $2\text{ }\mu\text{m}$. At 550 nm the single scattering albedo is 0.77 for a dry internal mixture particle.

The global and annual mean radiative forcing for an internal mixture is 0.10 W/m^2 as shown in Table 1. The higher degree of absorption has changed the sign from the external mixture forcing. The seasonal variation is large, and the global mean in July is 0.21 W/m^2 , whereas in January and October the values are close to zero. In the winter hemisphere the global mean internal forcing is very low or negative, as the relative humidity generally is higher during the winter than in the summer.

The annual mean spatial distribution is shown in Plate 6. The negative forcing over southern

Europe and eastern part of north America is much weaker compared to the external forcing, and in south east Asia the forcing has changed sign compared to the external forcing. Over western Asia the maximum forcing is localized with values close to 1.0 W/m^2 , and in the Arctic a strong heating of about 0.5 W/m^2 is found.

3.6. Sensitivity of the size of the soot particles

In the study of the internal mixture in the previous section the size of the particles are assumed to be the same as for ammonium sulfate, however the size of the internal mixture particles are larger than what we assumed for the size of the soot aerosols. Chylek and Wong (1995) have shown that the forcing depends on the size of the soot particles. We have therefore performed a sensitivity experiment.

New Mie calculations of soot aerosols with geometric mean radius of $0.05\text{ }\mu\text{m}$ show that the specific extinction coefficient above 550 nm , the asymmetry factor, and the single scattering albedo increase in comparison with results for the smaller soot particles. The resulting global and annual mean radiative forcing is 0.11 W/m^2 or 33% lower than for the geometric mean radius $0.0118\text{ }\mu\text{m}$. The external mixture forcing using geometric mean radius of $0.05\text{ }\mu\text{m}$ for both ammonium sulfate and soot is then -0.21 W/m^2 .

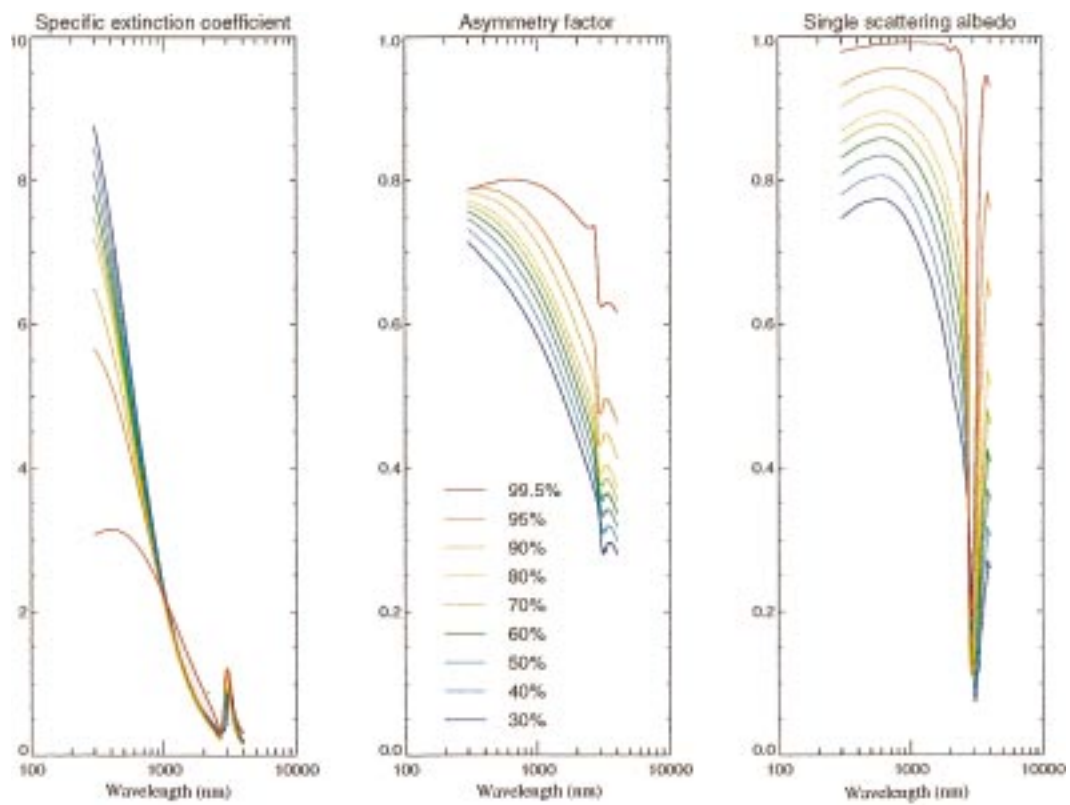


Fig. 3. As Fig. 1, but for an internal mixture of sulfate and soot.

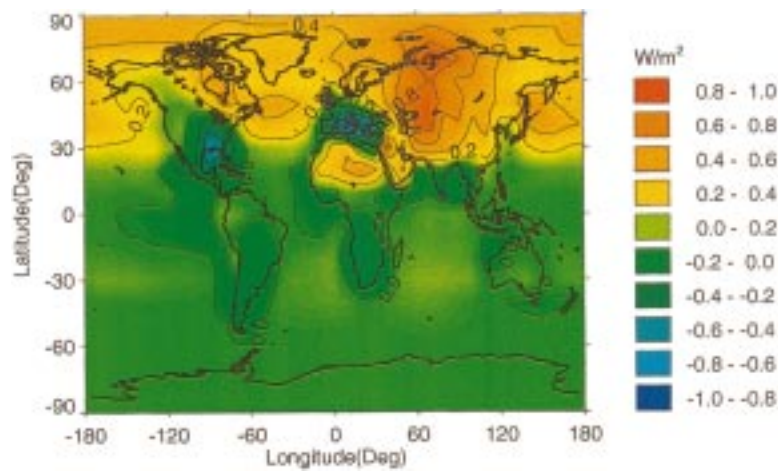


Plate 6. Yearly average radiative forcing due to an internal mixture of sulfate and soot aerosols.

4. Comparison with observations of single scattering albedo

The external and internal mixture calculations showed that a major part of the uncertainty in the radiative forcing by a mixture of sulfate and soot is connected to the single scattering albedo. This section will compare the surface single scattering albedo from the external and internal mixture Mie calculations with observed surface single scattering albedo. At present the number of observations is relatively low, with sparse spatial coverage. In addition the uncertainty in the observations is relatively large (Heintzenberg et al., 1997).

Table 2 shows observed single scattering albedo from Heintzenberg et al. (1997) in addition to our Mie calculated single scattering albedo from the external and internal mixtures. Fig. 4 compares our model results with the Heintzenberg et al. (1997) observations. Our model results are for a mixture of sulfate and soot particles, whereas the composition of the particles in the cases of observations is not well known. All values are surface single scattering albedo at 550 nm. Notice also that in the model results for the external and internal single scattering albedo the variation is

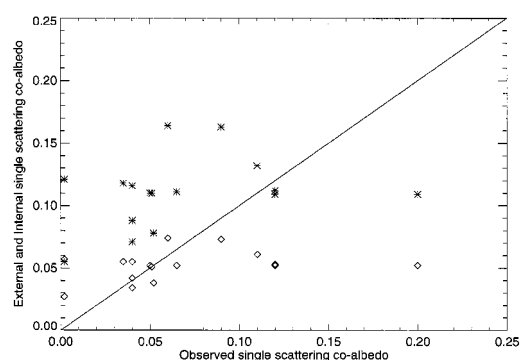


Fig. 4. Modelled external and internal mixture versus observed single scattering co-albedo. The values for an external mixture are shown with \diamond and for an internal mixture with $*$. The 1:1 relationship is marked with a line.

entirely due to variation in relative humidity, as we have kept the mass ratio constant, whereas in the observed cases, the mass ratio between soot and sulfate has probably varied, and the particles may even have a different composition. In most of the areas of these observations the model relative humidity is low, which was also the case in the actual observations. In spite of these caveats,

Table 2. Comparison of observed (Heintzenberg et al., 1997) and modelled (this work) single scattering albedo (ω)

Locations	Time	Obs	Model		
		ω	ω_{ext}	ω_{int}	
Barrow	annual	0.96	0.958	0.912	(71.2°N, 156.3°W)
Amundsen Scott	annual	0.965	0.945	0.882	(90°S)
Mauna Loa	June	0.95	0.948	0.890	(19.3°N, 155.4°W)
Mauna Loa	July	0.96	0.945	0.884	(19.3°N, 155.4°W)
Ny Ålesund	annual	0.948	0.962	0.922	(79°N, 12°E)
Kamchatka	May	0.88	0.947	0.888	(56°N, 160°E)
Equator	May	0.998	0.973	0.945	(0°, 100°E)
Wellington	June	0.88	0.948	0.891	(41.17°S, 174.47°E)
West Australia	June	0.998	0.943	0.879	(34.19°S, 115.09°E)
Tropical Atlantic Ocean	August	0.8	0.948	0.891	
Arctic	annual	0.96	0.966	0.929	
Alleghenny Mts.	summer	0.935	0.948	0.889	(38.3°N, 80°W)
Shenandoah	summer	0.949	0.949	0.890	(38°N, 78°W)
Mesa Verde	Annual	0.91	0.927	0.837	(37.1°N, 108.3°W)
Abastumani	Annual	0.89	0.939	0.868	(41.4°N, 42.5°E)
Anderson Mesa	Annual	0.94	0.926	0.836	(35.12°N, -111.38°W)

The model results are for external (ω_{ext}) as well as internal (ω_{int}) mixture.

in general the observations are in better agreement with modelled external mixture than internal mixture results. The disagreement between the observed values and the external mixture values are largest for low single scattering albedo (or a high single scattering co-albedo). The lowest possible value of the single scattering albedo for the external mixture is 0.903 under the assumption that the mass ratio between soot and sulfate is 0.075, as the single scattering albedo at 550 nm for soot and sulfate is 0.209 and 1.00, respectively.

Fig. 4 demonstrates that the external mixture single scattering co-albedo compare well with the majority of observations, but deviates significantly for 4 locations with high observed single scattering co-albedo and one location with low single scattering co-albedo. The internal mixture single scattering co-albedo is higher than the observations, except in 3 locations, and it is generally much higher than the observations.

The average values for the observed, and our modelled external and internal mixture single scattering albedo shown in Table 2 are 0.933, 0.948, and 0.890 respectively. Global and annual mean surface single scattering albedo at 550 nm calculated in this work for external and internal mixtures are 0.947 and 0.888, respectively.

5. Comparison with previous global radiative forcing estimates

5.1. Sulfate

Table 3 shows global estimates of the radiative forcing due to sulfate aerosols and the anthropogenic sulfate burden used in the radiative forcing calculations. Normalized forcing, which is the ratio between the radiative forcing and the anthropogenic sulfate burden, introduced by Boucher and Anderson (1995) and used in Feichter et al. (1997), is also shown in the table. Several estimates are performed; however, most of them use one of the distributions of Langner and Rodhe (1991), resulting from two different assumptions regarding SO₂ oxidation. The differences in the normalized forcing are somewhat smaller than the differences in radiative forcing estimates, especially between the newer estimates, among which the normalized forcing still varies by almost a factor of 2. This is not surprising, as there are presently large uncertainties in parameterizations of many processes controlling the radiative effects of sulfate particles. The normalized forcing depends e.g., on the seasonal and spatial variation in the sulfate distribution, aerosol optical properties, distribution and optical effects of relative humidity, direct radiative

Table 3. Comparison of global estimates of the radiative forcing due to sulfate

Work	Radiative forcing (W/m ²)	Sulfate burden (mg/m ²)	Normalized forcing (W/g)	Sulfate data
Charlson et al. (1991)	−0.60	2.0	−300	Langner and Rodhe (1991)
Kiehl and Briegleb (1993)	−0.28	1.76	−159	Langner and Rodhe (1991)
Taylor and Penner (1994)	−0.95	1.75 ^a	−543	Penner et al. (1994)
Kiehl and Rodhe (1995)	−0.66	3.23 ^b	−204	Pham et al. (1995)
Boucher and Anderson (1995)	−0.29	2.32	−125	Langner and Rodhe (1991)
Haywood and Shine (1995)	−0.34	1.8 ^c	−189	Langner and Rodhe (1991)
Haywood and Shine (1995)	−0.33	1.75 ^a	−189	Penner et al. (1994)
Haywood et al. (1997a)	−0.38	1.8 ^c	−211	Langner and Rodhe (1991)
Chuang et al. (1997)	−0.43	3.23 ^d		Chuang et al. (1997)
Feichter et al. (1997)	−0.35	2.23	−157	Feichter et al. (1997)
Graf et al. (1997)	−0.26	1.70	−153	Graf et al. (1997)
This work	−0.32	1.90	−168	Restad et al. (1997)

^aJ. Penner, personal communication (1997).

^bM. Pham, personal communication (1997).

^cJ. M. Haywood, personal communication (1997).

^dThe sulfate burden includes anthropogenic as well as natural sulfate. The contribution of the anthropogenic sulfate burden to the total sulfate burden varies between the models estimates, e.g., 69% in Pham et al. (1995), 64% in Restad et al. (1997), and 37% in Graf et al. (1997).

effects of sulfate aerosols in cloudy areas, as well as cloud distribution, surface albedo, and finally the radiative transfer code used in the calculations. The anthropogenic sulfate burden and the normalized forcing in this work are in both cases close to median values of the compared values in Table 3.

5.2. Soot

Two previous global estimates of the soot forcing are performed (Haywood and Shine, 1995; Haywood et al., 1997a). Haywood and Shine (1995) calculated only the clear sky soot forcing, while Haywood et al. (1997a) included clouds like in our calculations. They calculated 0.20 W/m^2 which compares well with the estimate of 0.16 W/m^2 in this work.

5.3. Sulfate and soot mixtures

Haywood et al. (1997a) have calculated the radiative forcing due to an external and internal mixture of sulfate and soot of -0.18 W/m^2 and -0.02 W/m^2 , respectively. Their estimates are lower than our results in both cases, most pronounced in the internal mixing case. In the case of external mixing it is worth noticing that the deviation between the results of the two models is larger in the separate sulfate and soot calculations than in the combined case. The higher internal mixture forcing calculated in this work compared to Haywood et al. (1997a) can probably mainly be explained by smaller temporal variations of relative humidities in our work, as well as different aerosol distribution and effect of clouds.

6. Summary

Based on a recent 3D CTM calculation of tropospheric sulfate, direct radiative forcings due to sulfate aerosols and soot aerosols are estimated. The resulting radiative forcing due to sulfate aerosols is -0.32 W/m^2 . Maximum forcing is found over southern Europe, where there are favourable atmospheric conditions for high sulfate forcing.

A linear mass ratio between fossil fuel soot and sulfate of 0.075 is assumed. This gives a radiative forcing from fossil fuel soot aerosols of 0.16 W/m^2 . Maximum soot forcing is found over eastern

Europe and the western part of Asia. At high latitudes in the northern hemisphere the soot forcing is relatively high due to high surface albedo. There are also other favourable regions for high soot forcing, mostly in the southern hemisphere. However, the soot amounts there are low. The calculated single scattering albedo for mixtures of sulfate and soot are compared with surface observations at 550 nm. The single scattering albedo using an external mixture of sulfate and soot is always above 0.9 in our calculations for a mass ratio between soot and sulfate of 0.075. Observed surface single scattering albedo in some regions is below 0.9, indicating that the linear relationship between soot and sulfate has several limitations or that at least some mixtures of sulfate and soot are not external. Another cause of deviations is that the observed single scattering albedo also reflects composition of particles other than sulfate and soot. The internal mixture single scattering albedo is generally lower than observed values, especially for high observed single scattering albedo.

The single scattering albedo is an important parameter in deciding the size of the radiative forcing due to the direct effect of tropospheric aerosols, and possibly also the sign. The difference in single scattering albedo is the main reason for the different radiative forcing of mixture of sulfate and soot as an external mixture (-0.16 W/m^2) and an internal mixture (0.10 W/m^2).

The uncertainty in the radiative forcing due to soot in a mixture with sulfate aerosols is not only connected to the type of mixture between them, but also to the soot distribution. We have assumed a linear mass relationship between soot and sulfate, which is uncertain both regarding the global distribution and the total global soot burden. In fact, the two CTM studies available (Liousse et al., 1996; Cooke et al., 1996) disagree by a factor of two on the soot burden. Future CTM calculations should in a consistent way include both sulfate and soot.

Finally, we would like to underline the fact that our calculations, as well as similar calculations published previously, suffer from significant uncertainties due to large uncertainties in the assumed spatial and temporal distribution of the aerosols as well as their size distribution and chemical composition.

7. Acknowledgments

We thank K. P. Shine for fruitful discussions which have given substantial input to this paper.

We also thank A. Dahlback for making a model available for us. This work has received support from the Regional Climate project under the Research Council of Norway.

REFERENCES

- Ackerman, T. P. and O. B. Toon, 1981. Absorption of visible radiation in atmosphere containing mixtures of absorbing and nonabsorbing particles. *Appl. Opt.* **20**, 3661–3668.
- Bates, T. S., B. K. Lamb, A. Guenther, J. Dignon and R. E. Stoiber, 1992. Sulfur emissions to the atmosphere from natural sources. *J. Atmos. Chem.* **14**, 315–357.
- Benkovitz, C. M., M. T. Scholtz, J. Pacyna, L. Tarrason, J. Dignon, E. C. Voldner, P. A. Spiro, J. A. Logan and T. E. Graedel, 1996. Global gridded inventories of anthropogenic emissions of sulfur and nitrogen. *J. Geophys. Res.* **101**, 29,239–29,253.
- Berntsen, T. K. and I. S. A. Isaksen, 1997. A global three-dimensional chemical transport model for the troposphere, 1. Model description and CO₂ and ozone results. *J. Geophys. Res.* **102**, 21,239–21,280.
- Berntsen, T. K., I. S. A. Isaksen, G. Myhre, J. S. Fuglestad, F. Stordal, T. Alsosvik Larsen, R. S. Freckleton and K. P. Shine, 1997. Effects of anthropogenic emissions on tropospheric ozone and its radiative forcing. *J. Geophys. Res.* **102**, 28,101–28,126.
- Boucher, O. and T. L. Anderson, 1995. General circulation model assessment of the sensitivity of direct climate forcing by anthropogenic sulfate aerosols to aerosol size and chemistry. *J. Geophys. Res.* **100**, 26,117–26,134.
- Charlson, R. J., J. Langner, H. Rodhe, C. B. Leovy and S. G. Warren, 1991. Perturbation of the northern hemisphere radiative balance by backscattering from anthropogenic sulfate aerosols. *Tellus* **43A**, 152–163.
- Chuang, C. C., J. E. Penner, K. E. Taylor, A. S. Grossman and J. J. Walton, 1997. An assessment of the radiative effects of anthropogenic sulfate. *J. Geophys. Res.* **102**, 3761–3778.
- Chylek, P. and J. Wong, 1995. Effect of absorbing aerosols on global radiation budget. *Geophys. Res. Lett.* **22**, 929–931.
- Coakley, J. A. Jr., R. D. Cess and F. B. Yurevich, 1983. The effect of tropospheric aerosols on the earth's radiation budget: a parameterization for climate models. *J. Atmos. Sci.* **40**, 116–138.
- Cooke, W. F. and J. J. N. Wilson, 1996. A global black carbon model. *J. Geophys. Res.* **101**, 19,395–19,409.
- Feichter, J., E. Kjellstrom, H. Rodhe, F. Dentener, J. Lelieveld and G.-J. Roelofs, 1996. Simulation of the tropospheric sulfur cycle in a global climate model. *Atmos. Environ.* **30**, 1693–1707.
- Feichter, J., U. Lohmann and I. Schult, 1997. The atmospheric sulfur cycle in ECHAM-4 and its impact on the short-wave radiation. *Climate Dynamics* **13**, 235–246.
- Fitzgerald, J. W. 1975. Approximation formulas for the equilibrium size of an aerosol particle as a function of its dry size and composition and the ambient relative humidity. *J. Appl. Meteor.* **14**, 1044–1049.
- Frohlich, C. and J. London (eds.) 1986. *Revised instruction manual on radiation instruments and measurements*. WCRP Pub. Series no. 7., WMO/TD. no. 149, 140 pp.
- Graf, H.-F., J. Feichter and B. Langmann, 1997. Volcanic sulfur emissions: estimates of source strength and its contribution to the global sulfate distribution. *J. Geophys. Res.* **102**, 10,727–10,738.
- Hansen, J., M. Sato and R. Ruedy, 1997. Radiative forcing and climate response. *J. Geophys. Res.* **102**, 6831–6864.
- Haywood, J. M. and K. P. Shine, 1995. The effect of anthropogenic sulfate and soot aerosol on the clear sky planetary radiation budget. *J. Geophys. Res.* **22**, 603–606.
- Haywood, J. M. and K. P. Shine, 1997. Multi-spectral calculations of the direct radiative forcing of tropospheric sulphate and soot aerosols using a column model. *Q. J. R. Meteorol. Soc.* **123**, 1907–1930.
- Haywood, J. M., D. L. Roberts, A. Slingo, J. M. Edwards and K. P. Shine, 1997a. General circulation model calculations of the direct radiative forcing by anthropogenic sulfate and fossil-fuel soot aerosol. *J. Clim.* **10**, 1562–1577.
- Haywood, J. M., V. Ramaswamy and L. J. Donner, 1997b. A limited-area-model case study of the effects of sub-grid scale variations in relative humidity and cloud upon the direct radiative forcing of sulfate aerosol. *Geophys. Res. Lett.* **24**, 143–146.
- Heintzenberg, J., R. J. Charlson, A. D. Clarke, C. Liou, V. Ramaswamy, K. P. Shine, M. Wendisch and G. Helas, 1997. Measurements and modelling of aerosol single-scattering albedo: progress, problems and prospects. *Beitr. Phys. Atmosph.* **70**, 249–263.
- Intergovernmental Panel on Climate Change (IPCC) 1990. *Climate change: the IPCC scientific assessment*, edited by J. T. Houghton, G. J. Jenkins and J. J. Ephraums, 1990. Cambridge University Press, Cambridge, UK.
- Intergovernmental Panel on Climate Change (IPCC) 1995. *Climate change 1995: the science of climate change*, edited by J. T. Houghton, L. G. Meira Filho, B. A. Callander, N. Harris, A. Kattenberg and K. Maskell. Cambridge University Press, Cambridge, UK.
- Kiehl, J. T. and B. P. Briegleb, 1993. The relative roles

- of sulfate aerosols and greenhouse gases in climate forcing. *Science* **260**, 311–314.
- Kiehl, J. T. and H. Rodhe, 1995. Modeling geographical and seasonal forcing due to aerosols. In: *Aerosol forcing of climate*, R. J. Charlson and J. Heintzenberg (eds). John Wiley, Chichester, 281–296.
- Langner, J. and H. Rodhe, 1991. A global three-dimensional model of the tropospheric sulfur cycle. *J. Atmos. Chem.* **13**, 225–263.
- Lacis, A. A. and M. I. Mishchenko, 1995. Climate forcing, climate sensitivity, and climate response: a radiative modeling perspective on atmospheric aerosols. In: *Aerosol forcing of climate*, R. J. Charlson and J. Heintzenberg (eds). John Wiley, Chichester, 11–42.
- Liang, X.-Z. and W.-C. Wang, 1995. A GCM study of the climatic effect of 1979–1992 ozone trend. In: *Atmospheric ozone as a climate gas*, edited by W.-C. Wang and I. S. A. Isaksen. NATO ASI Ser., Springer-Verlag, New York.
- Liousse, C., J. E. Penner, C. Chuang, J. J. Walton, H. Eddleman and H. Cachier, 1996. A global three-dimensional model study of carbonaceous aerosols. *J. Geophys. Res.* **101**, 19,411–19,432.
- Myhre, G. and F. Stordal, 1997. Role of spatial and temporal variations in the computation of radiative forcing and GWP. *J. Geophys. Res.* **102**, 11,181–11,200.
- Nemesure, S., R. Wagener and S. E. Schwartz, 1995. Direct short-wave forcing of climate by anthropogenic sulfate aerosols: sensitivity to particle size, composition and relative humidity. *J. Geophys. Res.* **100**, 26,105–26,116.
- Penner, J. E., C. S. Atherton and T. E. Graedel, 1994. Global emissions and models of photochemically active compounds. In: *Global atmospheric-biospheric chemistry*, edited by R. G. Prinn, pp. 223–247. Plenum, New York.
- Pham M., J.-F. Müller, G. P. Brasseur, C. Granier and G. Mégie, 1995. A three-dimensional study of the tropospheric sulfur cycle. *J. Geophys. Res.* **100**, 26,061–26,092.
- Pilinis, C., S. N. Pandis and J. H. Seinfeld, 1995. Sensitivity of direct climate forcing by atmospheric aerosols to aerosol size and composition. *J. Geophys. Res.* **100**, 18,739–18,754.
- Ramaswamy, V. and C.-T. Chen, 1997. Climate forcing-response relationships for greenhouse and short-wave radiative perturbations. *Geophys. Res. Lett.* **24**, 667–670.
- Restad, K., I. S. A. Isaksen and T. K. Berntsen, 1998. Global distribution of sulfate particles in the troposphere: Study with a 3-dimensional model. *Atmos. Environ.*, in press.
- Rodhe, H. and I. S. A. Isaksen, 1980. Global distribution of sulfur compounds in the troposphere estimated in a height/latitude transport model. *J. Geophys. Res.* **85**, 7401–7409.
- Rossow, W. B. and R. A. Schiffer, 1991. ISCCP cloud data products. *Bull. Am. Meteorol. Soc.* **72**, 2–20.
- Rothman, L. S. et al. 1992. The HITRAN molecular database: Editions of 1991 and 1992. *J. Quant. Spectrosc. Radiat. Transfer* **48**, 469–507.
- Stamnes, K., S.-C. Tsay, W. Wiscombe and K. Jayaweera, 1988. A numerically stable algorithm for discrete-ordinate-method radiative transfer in multiple scattering and emitting layered media. *Appl. Opt.* **27**, 2502–2509.
- Stoiber, R. E., S. N. Williams and B. Huebert, 1987. Annual contribution of sulfur dioxide to the atmosphere by volcanoes. *J. Volcanol. Geotherm.* **33**, 1–8.
- Taylor, K. E. and J. E. Penner, 1994. Response of the climate system to atmospheric aerosols and greenhouse gases. *Nature* **369**, 734–737.
- Toon, O. B., J. B. Pollack and B. N. Khare, 1976. The optical constants of several atmospheric aerosol species, ammonium sulphate, aluminium oxide, and sodium chloride. *J. Geophys. Res.* **81**, 5733–5748.
- WCP, 1986. *A preliminary cloudless standard atmosphere for radiation computation*. World Climate Programme, Rep. WCP-112.
- World Meteorological Organization (WMO), 1985. *Global ozone research and monitoring project*, rep. **16**: Atmospheric Ozone.